Journal of Zhejiang University-SCIENCE C (Computers & Electronics)
ISSN 1869-1951 (Print); ISSN 1869-196X (Online)
www.zju.edu.cn/jzus; www.springerlink.com
E-mail: jzus@zju.edu.cn

Saturated output feedback tracking control for robot manipulators via fuzzy self-tuning*

Hua-shan LIU[†1,2], Shi-qiang ZHU[†‡1], Zhang-wei CHEN[1]
([1]*State Key Lab of Fluid Power Transmission and Control, Zhejiang University, Hangzhou 310027, China*)
([2]*College of Information Science and Technology, Donghua University, Shanghai 201620, China*)
[†]E-mail: watson683@163.com; sqzhu@zju.edu.cn

Received Dec. 18, 2009; Revision accepted Apr. 12, 2010; Crosschecked Nov. 12, 2010

Abstract: This paper concerns the problem of output feedback tracking (OFT) control with bounded torque inputs of robot manipulators, and proposes a novel saturated OFT controller based on fuzzy self-tuning proportional and derivative (PD) gains. First, aiming to accomplish the whole closed-loop control with only position measurements, a linear filter is involved to generate a pseudo velocity error signal. Second, different from previous strategies, the arctangent function with error-gain is applied to ensure the boundedness of the torque control input, and an explicit system stability proof is made by using the theory of singularly perturbed systems. Moreover, a fuzzy self-tuning PD regulator, which guarantees the continuous stability of the overall closed-loop system, is added to obtain an adaptive performance in tackling the disturbances during tracking control. Simulation showed that the proposed controller gains more satisfactory tracking results than the others, with a better dynamic response performance and stronger anti-disturbance capability.

Key words: Robot, Tracking systems, Bounded torque input, Fuzzy control, Output feedback
doi:10.1631/jzus.C0910772 **Document code:** A **CLC number:** TP24

1 Introduction

Recently, the issue of trajectory tracking control with bounded torque inputs has aroused increasing interest in robot motion control research, especially the output feedback tracking (OFT) control without velocity measurements (Loria and Nijmeijer, 1998; Santibanez and Kelly, 2001; Moreno-Valenzuela *et al*., 2008a).

The first saturated OFT controller was proposed by Loria and Nijmeijer (1998), where the hyperbolic tangent function was invoked in the control law to ensure the boundedness of the torque input to each joint actuator of robot, while a nonlinear filter containing only the position error variable was applied to create a pseudo velocity error signal. The semi-global stability of the system was achieved by using sufficiently large observer gains, although the stability analysis was expressed in a rather complicated manner. This scheme exerted an important effect on subsequent research. Santibanez and Kelly (2001) made a supplementary development to this scheme by considering the viscous friction in the robot joints, and proved that the global asymptotic stability can be assured if a large enough viscous friction damping is present. Moreno-Valenzuela *et al*. (2008a; 2008b) introduced the stability theory of singularly perturbed systems to make an explicit stability proof of the OFT controller and proposed a general expression of a class of saturated OFT controllers. Motivated by this, and based on the theory of singularly perturbed systems, Liu and Zhu (2009) designed a more generalized saturated OFT controller with a broader relationship between the variable matrix and the error-gain matrix, and applied a linear filter to generate the

‡ Corresponding author
* Project (No. 2008C21106) supported by the Science and Technology Foundation of Zhejiang Province, China

pseudo velocity error signal. With respect to the theory of singularly perturbed systems, it is remarkable that it was first used to tackle OFT control by Burkov (1998), but without mentioning the torque saturation problem.

In addition, most of the saturated OFT strategies besides those mentioned above have fixed proportional and derivative (PD) gains, which must be selected by trial and error for each demanded task, with considering many complicated factors, e.g., the stability of the dynamic systems, saturation constraints, and the initial position tracking errors. More recently, some studies have been reported to regulate the fixed gains with explicit formulas (Meza *et al*., 2007; Hernandez-Guzman *et al*., 2008; Santibanez *et al*., 2008), but they are still limited to improving the tracking performance.

It is well known that, in closed-loop control, for large position tracking errors, small enough gains should be selected so as not to cause a huge overshoot or even destroy the system stability. Meanwhile, as the tracking error becomes smaller, larger gains will be necessary to obtain good accuracy (Llama *et al*., 2001). Therefore, to gain a more satisfactory control performance, making the PD gains self-tuning online is necessary. Some previous studies have contributed to solving this problem for tracking control (Llama *et al*., 1998; 1999; Santibanez *et al*., 2000; Li *et al*., 2001), but few of them considered torque saturation. By taking into account the torque saturation problem, Llama *et al*. (2001) proposed a saturated tracking controller equipped with a fuzzy PD regulator, but it was not a strict OFT controller (which needs velocity measurements), and the boundedness of the control signals was assured by limiting the range of PD gains, which can be gained only in the situations where maximum position and velocity errors are known beforehand. Another approach was proposed by Santibanez *et al*. (2005), where a novel fuzzy controller for bounded control was introduced, but it aimed only to solve the set-point control problem. It seems that continuous stability analysis becomes more complicated when the PD gains are self-tuning during OFT control, and few studies have presented a proof of global asymptotic stability (Andrieu and Praly, 2009) for output feedback systems, or even a proof of achieving simultaneously both stability and good performance (Hernandez-Guzman *et al*., 2008).

In this paper, a novel saturated controller with an error-gain contained arctangent function in the control law is designed. To the best of our knowledge, we are the first to invoke arctangent as the saturation function in saturated tracking control. As a second contribution, a fuzzy PD regulator is applied to make the PD gains self-tuning online as the position error varies, which is vital for anti-disturbances; more importantly, continuous semi-global exponential stability of the whole closed-loop system is guaranteed under sufficient restrictions during the adaptive process.

Notations: throughout this paper, $\|\boldsymbol{x}\|$ and $\|\boldsymbol{X}\|$ stand for the Euclidean norm of vector $\boldsymbol{x}$ and induced L_2 norm of matrix $\boldsymbol{X}$, respectively; x_{m} and x_{M} denote the minimum and maximum values of variable x, respectively; $\lambda_{\mathrm{m}}\{\boldsymbol{X}\}$ and $\lambda_{\mathrm{M}}\{\boldsymbol{X}\}$ stand for the smallest and largest eigenvalues of matrix $\boldsymbol{X}$, respectively.

2 Dynamic model and properties

2.1 Robot dynamics

The dynamics of a rigid serial n-link robot manipulator with revolute joints can be written as

$$\boldsymbol{M}(\boldsymbol{q})\ddot{\boldsymbol{q}}+\boldsymbol{C}(\boldsymbol{q},\dot{\boldsymbol{q}})\dot{\boldsymbol{q}}+\boldsymbol{G}(\boldsymbol{q})+\boldsymbol{F}_{\mathrm{v}}\dot{\boldsymbol{q}}=\boldsymbol{\tau}, \tag{1}$$

where $\boldsymbol{q}\in\mathbb{R}^n$ denotes the joint angle vector, $\boldsymbol{M}(\boldsymbol{q})\in\mathbb{R}^{n\times n}$ represents the inertia matrix, $\boldsymbol{C}(\boldsymbol{q},\dot{\boldsymbol{q}})\in\mathbb{R}^{n\times n}$ is the centripetal-Coriolis matrix , $\boldsymbol{G}(\boldsymbol{q})\in\mathbb{R}^n$ is the vector of gravity effect, $\boldsymbol{F}_{\mathrm{v}}=\mathrm{diag}\{f_{\mathrm{v}1}, f_{\mathrm{v}2}, \ldots, f_{\mathrm{v}n}\}\in\mathbb{R}^{n\times n}$ ($f_{\mathrm{v}i}>0$, $i=1, 2, \ldots, n$) is the viscous friction coefficient matrix, and $\boldsymbol{\tau}\in\mathbb{R}^n$ is the vector of the input torque.

2.2 Properties on the dynamic model

Some useful properties (Kelly and Santibanez, 2005) of the robot dynamic model (1) are listed below.

P1. The inertia and centripetal-Coriolis matrices satisfy the following skew symmetric relationship:

$$\boldsymbol{x}^{\mathrm{T}}[\dot{\boldsymbol{M}}(\boldsymbol{q})-2\boldsymbol{C}(\boldsymbol{q},\dot{\boldsymbol{q}})]\boldsymbol{x}=0, \tag{2}$$

$$\dot{\boldsymbol{M}}(\boldsymbol{q})=\boldsymbol{C}(\boldsymbol{q},\dot{\boldsymbol{q}})+\boldsymbol{C}(\boldsymbol{q},\dot{\boldsymbol{q}})^{\mathrm{T}}. \tag{3}$$

P2. The inertia matrix $\boldsymbol{M}(\boldsymbol{q})$ is symmetric, positive definite, and satisfies the following inequalities:

$$\lambda_{\rm m}\{\boldsymbol{M}(\boldsymbol{q})\}\|\boldsymbol{x}\|^2 \le \boldsymbol{x}^{\rm T}\boldsymbol{M}(\boldsymbol{q})\boldsymbol{x} \le \lambda_{\rm M}\{\boldsymbol{M}(\boldsymbol{q})\}\|\boldsymbol{x}\|^2. \quad (4)$$

P3. $\forall \boldsymbol{x}, \boldsymbol{y}, \boldsymbol{z}\in\mathbb{R}^n$, the centripetal-Coriolis matrix satisfies the following transformations:

$$\boldsymbol{C}(\boldsymbol{x},\boldsymbol{y})\boldsymbol{z} = \boldsymbol{C}(\boldsymbol{x},\boldsymbol{z})\boldsymbol{y}, \quad (5)$$

$$\boldsymbol{C}(\boldsymbol{x},\boldsymbol{y}+\boldsymbol{z}) = \boldsymbol{C}(\boldsymbol{x},\boldsymbol{y}) + \boldsymbol{C}(\boldsymbol{x},\boldsymbol{z}). \quad (6)$$

P4. The centripetal-Coriolis gravity terms can be bounded in the following manner:

$$\|\boldsymbol{C}(\boldsymbol{q},\dot{\boldsymbol{q}})\| \le k_{\rm C}\|\dot{\boldsymbol{q}}\|, \quad \|\boldsymbol{G}(\boldsymbol{q})\|_{\rm M} \le k_{\rm G}. \quad (7)$$

3 Arctangent saturation function

The most common strategy to ensure the boundedness of the torque control inputs in previous studies was applying the hyperbolic tangent function, tanh, in the control law (Loria and Nijmeijer 1998; Llama *et al*., 2001; Santibanez and Kelly, 2001; Moreno-Valenzuela *et al*., 2008a; 2008b; Santibanez *et al*., 2008). In this work, considering that the arctangent function also features saturation (Fig. 1), we thereby contribute a new saturated OFT controller.

We define $\text{Atan}(\boldsymbol{\varDelta x})=[\text{atan}(\sigma_1 x_1), \text{atan}(\sigma_2 x_2), \ldots, \text{atan}(\sigma_n x_n)]^{\rm T}\in\mathbb{R}^n$, where $\boldsymbol{x}=[x_1, x_2, \ldots, x_n]^{\rm T}\in\mathbb{R}^n$, $\boldsymbol{\varDelta}=\text{diag}\{\sigma_1, \sigma_2, \ldots, \sigma_n\}\in\mathbb{R}^{n\times n}$, $\sigma_i\ge1$, $i=1, 2, \ldots, n$, and use $\sigma_{\rm m}$ ($\sigma_{\rm M}$) to denote the minimum (maximum) value of σ_i. Some useful properties of the arctangent function are as follows:

Q1. $\text{atan}(\sigma_i x_i)$ is a monotone increasing function in a real domain; i.e., $\dfrac{\partial\text{atan}(\sigma_i x_i)}{\partial x_i}\ge 0$, $\forall x_i\in\mathbb{R}$, and there always exists $\text{atan}(\sigma_i x_i)\cdot x_i\ge0$, if and only if $x_i=0$, $\text{atan}(\sigma_i x_i)\cdot x_i=0$.

Q2. $|\text{atan}(\sigma_i x_i)|<\pi/2$ and $\|\text{Atan}(\boldsymbol{\varDelta x})\|<\sqrt{n}\pi/2$ are satisfied $\forall x_i\in\mathbb{R}$.

Q3. $\forall\boldsymbol{x}\in\mathbb{R}^n$, there exists $\sigma_{\rm M}\|\boldsymbol{x}\|\ge\|\text{Atan}(\boldsymbol{\varDelta x})\|$.

Q4. $\text{Atan}(\boldsymbol{\varDelta x})$ is continuously differentiable and satisfies $\lambda_{\rm M}\left\{\dfrac{\partial\text{Atan}(\boldsymbol{\varDelta x})}{\boldsymbol{\varDelta}\partial\boldsymbol{x}}\right\}\le1 \ \ \forall\boldsymbol{x}\in\mathbb{R}^n$.

Q5. $\forall\boldsymbol{x}\in\Omega_\eta$, $\Omega_\eta=\{\boldsymbol{x}\in\mathbb{R}^n: \|\boldsymbol{x}\|\le\eta\}$, where $\eta>0$ is arbitrarily large, there exists a large enough constant $\alpha\ge\dfrac{\sigma_{\rm m}\eta}{\text{atan}(\sigma_{\rm m}\eta)}>1$ to satisfy $\alpha\|\text{Atan}(\boldsymbol{\varDelta x})\|\ge\sigma_{\rm m}\|\boldsymbol{x}\|$.

Q6. $\forall\boldsymbol{x}\in\Omega_\eta$, there exists a large enough constant $\beta\ge\left\{\sigma_{\rm M}\eta\,\text{atan}(\sigma_{\rm M}\eta)-\dfrac{1}{2}\ln\left[1+(\sigma_{\rm M}\eta)^2\right]\right\}\Big/\left[\text{atan}(\sigma_{\rm M}\eta)\right]^2$ to satisfy $\dfrac{1}{2}\|\text{Atan}(\boldsymbol{\varDelta x})\|^2\le\sum_{i=1}^{n}\sigma_i\int_0^{x_i}\text{atan}(\sigma_i x_i)\text{d}x_i\le\beta\|\text{Atan}(\boldsymbol{\varDelta x})\|^2$.

As shown in Fig. 1, in response to the increasing values of σ_i, the zero-crossing slope of $\text{atan}(\sigma_i x_i)$ steeply increases and rapidly approaches saturation. Function atan has a wider range of $(-\pi/2, \pi/2)$ and behaves in a more moderate approach to saturation for the same value of σ_i than function tanh with a range of $(-1, 1)$. These features have proven helpful in improving the tracking performance (Liu and Zhu, 2009).

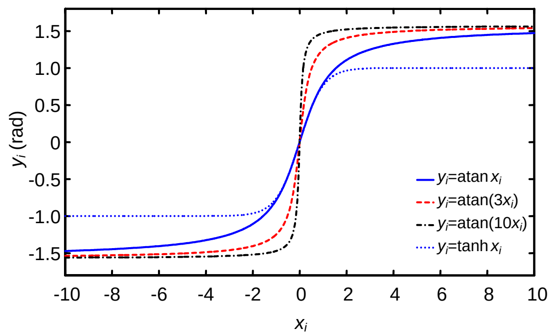

Fig. 1 Function curves of atan and tanh

4 Control design and stability analysis

By applying the saturation properties about the arctangent function listed above, the first-order linear filter, and fuzzy strategies, a novel saturated OFT controller via fuzzy self-tuning is designed. Then, an explicit stability analysis of the overall closed-loop control system is presented.

4.1 Control goal

Noting that the torque outputs of actuators in each joint of robot are limited, we aim to design an OFT controller with bounded inputs $|\tau_i|<\tau_{i\rm M}$ ($i=1, 2, \ldots, n$), to make the actual joint displacement $\boldsymbol{q}(t)\in\mathbb{R}^n$ converge asymptotically to the desired joint displacements $\boldsymbol{q}_{\rm d}(t)\in\mathbb{R}^n$, where τ_i is the control input to the ith joint actuator, whose upper bound of the torque output is $\tau_{i\rm M}$. Then, the control goal can be written as

$$\forall\, \boldsymbol{e}(0) \in \mathbb{R}^n, \quad \lim_{t\to\infty} \boldsymbol{e}(t) = \boldsymbol{0}, \tag{8}$$

where $\boldsymbol{e}(t)=\boldsymbol{q}_d(t)-\boldsymbol{q}(t)$ is the position tracking error.

In addition, we assume $\boldsymbol{q}_d(t)$ and its first two derivatives are bounded $\forall t\geq 0$:

$$\|\boldsymbol{q}_d(t)\| \leq \|\boldsymbol{q}_d(t)\|_M, \tag{9}$$
$$\|\dot{\boldsymbol{q}}_d(t)\| \leq \|\dot{\boldsymbol{q}}_d(t)\|_M, \tag{10}$$
$$\|\ddot{\boldsymbol{q}}_d(t)\| \leq \|\ddot{\boldsymbol{q}}_d(t)\|_M. \tag{11}$$

4.2 Saturated control law

The block diagram of the proposed saturated OFT controller is shown in Fig. 2.

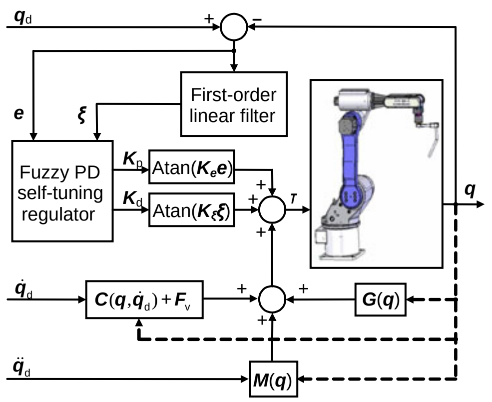

Fig. 2 Block diagram of the proposed output feedback tracking (OFT) controller

For convenience, we use $\boldsymbol{K}_p$, $\boldsymbol{K}_d$, $\boldsymbol{M}$, $\boldsymbol{C}$, $\boldsymbol{C}_d$, and $\boldsymbol{G}$ to represent $\boldsymbol{K}_p(\boldsymbol{e}, \xi)$, $\boldsymbol{K}_d(\boldsymbol{e}, \xi)$, $\boldsymbol{M}(\boldsymbol{q})$, $\boldsymbol{C}(\boldsymbol{q}, \dot{\boldsymbol{q}})$, $\boldsymbol{C}(\boldsymbol{q}, \dot{\boldsymbol{q}}_d)$, and $\boldsymbol{G}(\boldsymbol{q})$, respectively. Then the control law is given as

$$\begin{aligned}\boldsymbol{\tau} = &\boldsymbol{K}_p \mathrm{Atan}(\boldsymbol{K}_e \boldsymbol{e}) + \boldsymbol{K}_d \mathrm{Atan}(\boldsymbol{K}_\xi \boldsymbol{\xi}) \\ &+ \boldsymbol{M}\ddot{\boldsymbol{q}}_d + (\boldsymbol{C}_d + \boldsymbol{F}_v)\dot{\boldsymbol{q}}_d + \boldsymbol{G},\end{aligned} \tag{12}$$

where $\boldsymbol{\xi}\in\mathbb{R}^n$ is the man-made pseudo velocity error. $\boldsymbol{K}_p=\mathrm{diag}\{k_{p1}(\boldsymbol{e}, \boldsymbol{\xi}), k_{p2}(\boldsymbol{e}, \boldsymbol{\xi}), \ldots, k_{pn}(\boldsymbol{e}, \boldsymbol{\xi})\}\in\mathbb{R}^{n\times n}$ is the diagonal matrix of the proportional gain, $\boldsymbol{K}_d=\mathrm{diag}\{k_{d1}(\boldsymbol{e}, \boldsymbol{\xi}), k_{d2}(\boldsymbol{e}, \boldsymbol{\xi}), \ldots, k_{dn}(\boldsymbol{e}, \boldsymbol{\xi})\}\in\mathbb{R}^{n\times n}$ is the diagonal matrix of the derivative gain. $\boldsymbol{K}_e\in\mathbb{R}^{n\times n}$ is the diagonal matrix of the position error, and $\boldsymbol{K}_\xi\in\mathbb{R}^{n\times n}$ is the diagonal matrix of the velocity error. $k_{pi}(\boldsymbol{e}, \boldsymbol{\xi})$, $k_{di}(\boldsymbol{e}, \boldsymbol{\xi})>0$, k_{ei}, $k_{\xi i}\geq 1$, $i=1, 2, \ldots, n$.

The man-made signal $\boldsymbol{\xi}$ satisfies: $\dot{\boldsymbol{r}}=\boldsymbol{U}\boldsymbol{\xi}$, $\boldsymbol{\xi}=\boldsymbol{U}\boldsymbol{e}-\boldsymbol{r}$, where $\boldsymbol{U}=\mathrm{diag}\{\mu_1, \mu_2, \ldots, \mu_n\}\in\mathbb{R}^{n\times n}$, $\mu_i>0$, $i=1, 2, \ldots, n$.

Thus, we have

$$\dot{\boldsymbol{\xi}} = \boldsymbol{U}(\dot{\boldsymbol{e}} - \boldsymbol{\xi}). \tag{13}$$

Obviously, Eq. (13) is a linear filter eliminating the measurements of velocity. $\boldsymbol{r}$ is an auxiliary variable introduced to divide the filter into two implementable parts.

Therefore, by properties P2, P4, Q2, and Eqs. (10) and (11), the boundedness of control input can be assured with satisfying the following inequality:

$$\begin{aligned}\tau_{iM} > \sup|\tau_i| = &\frac{\pi}{2}\sup(k_{pi}+k_{di}) + \|\boldsymbol{M}_i\|_M \|\ddot{\boldsymbol{q}}_d\|_M \\ &+ \|\boldsymbol{C}_{di}\|_M \|\dot{\boldsymbol{q}}_d\|_M + |G_i|_M + f_{vi}|\dot{q}_{di}|_M,\end{aligned} \tag{14}$$

where $\boldsymbol{M}_i$, $\boldsymbol{C}_{di}$, and G_i denote the ith rows of $\boldsymbol{M}$, $\boldsymbol{C}_d$, and $\boldsymbol{G}$, respectively.

Some systematic works (Park and Choi, 1995; Hu *et al.*, 2008; Yoon *et al.*, 2008; Dai *et al.*, 2009) have contributed to evolving the problem of saturated control for linear or nonlinear dynamic systems in recent years, which may exert a strong influence on the saturated OFT control.

4.3 Fuzzy self-tuning regulator

A fuzzy PD self-tuning regulator, as shown in Figs. 2 and 3, is designed to enhance the robustness and the dynamic response ability of the whole closed-loop tracking system.

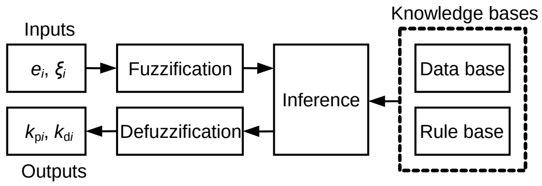

Fig. 3 Structure of the fuzzy proportional and derivative (PD) self-tuning regulator

4.3.1 Fuzzification

The physical universe of discourse of e_i, ξ_i, k_{pi}, and k_{di} can all be partitioned into the same fuzzy sets {NB, NM, NS, Z, PS, PM, PB}, matching along with the integer universe of discourse: {−3, −2, −1, 0, 1, 2, 3}. The membership function of e_i, ξ_i, k_{pi}, and k_{di} are chosen to be the same (Fig. 4): asymmetrical polynomial curve based membership functions for NB and PB, while triangular membership functions for NM, NS, Z, PS, and PM.

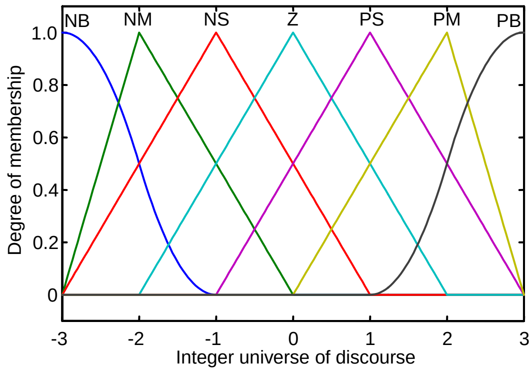

Fig. 4 Membership functions for e_i, ξ_i, k_{pi}, and k_{di}

4.3.2 Knowledge base and inference

The knowledge base consists of two parts: the data base and the rule base. The data base provides membership functions related values of variables in fuzzy sets for inference, while the rule base offers the rules for the inference engine, which is chosen as the Mamdani-type.

Note that, to reduce the computational effort and gain real-time performance of fuzzy tuning, the rules should be as simple as possible. Therefore, we make an approximate treatment, neglecting the coupling relationship among the joints. The rules for tuning PD gains of each robot joint in the rule base are given as

IF e_i is A_i AND ξ_i is B_i
THEN k_{pi} is C_i AND k_{di} is D_i,

where A_i, B_i, C_i, and D_i are certain elements of linguistic terms such as {NB, NM, NS, Z, PS, PM, PB}.

4.3.3 Defuzzification

The centroid method is selected in the defuzzification of outputs. It can be simply expressed as

$$k = \sum_{i=1}^{n} k_i u_i \Big/ \sum_{i=1}^{n} u_i , \tag{15}$$

where k, as the output of the fuzzy regulator, denotes k_{pi} or k_{di}, k_i is the element in physical universe of discourse of k, and u_i is the degree of membership of k_i.

Note that, when selecting proper PD gains, it is difficult to achieve simultaneously system stability and good performance (Hernandez-Guzman *et al.*, 2008). However, in this study, after the stability analysis in the following subsection, some constraint conditions to the output values of the fuzzy PD self-tuning regulator will be extracted to ensure both the continuous semi-global asymptotic (exponential) stability and satisfactory tracking results of the system.

4.4 Analysis of system stability

In this subsection, the theory of singularly perturbed systems (Khalil, 2007) is applied to give an explicit and strict stability analysis of the proposed OFT controller (Moreno-Valenzuela *et al.*, 2008a; 2008b).

Ordering $\boldsymbol{x}=[\boldsymbol{e}^{\mathrm{T}}\ \dot{\boldsymbol{e}}^{\mathrm{T}}]^{\mathrm{T}}$, and substituting Eq. (12) into Eq. (1), we obtain

$$\dot{\boldsymbol{x}}_1 = \dot{\boldsymbol{e}}, \tag{16}$$

$$\begin{aligned}\dot{\boldsymbol{x}}_2 = \ddot{\boldsymbol{e}} = -\boldsymbol{M}^{-1}[&\boldsymbol{K}_{\mathrm{p}}\mathrm{Atan}(\boldsymbol{K}_{\boldsymbol{e}}\boldsymbol{e}) \\ &+ \boldsymbol{K}_{\mathrm{d}}\mathrm{Atan}(\boldsymbol{K}_{\xi}\boldsymbol{\xi}) + (\boldsymbol{C}+\boldsymbol{C}_{\mathrm{d}}+\boldsymbol{F}_{\mathrm{v}})\dot{\boldsymbol{e}}].\end{aligned} \tag{17}$$

Order $\boldsymbol{z}=\boldsymbol{\xi}$, $\mu_i=\mu$, and $\varepsilon=1/\mu$, where μ_i (i=1, 2, …, n) is as described in Section 4.2. Then Eq. (13) is written as

$$\varepsilon\dot{\boldsymbol{z}} = \varepsilon\frac{\mathrm{d}\boldsymbol{\xi}}{\mathrm{d}t} = \dot{\boldsymbol{e}} - \boldsymbol{\xi}. \tag{18}$$

We can easily find that Eq. (18) has an isolated root $\boldsymbol{\xi} = \dot{\boldsymbol{e}}$. Then the system (16), (17), and (18) has the same form as that of the nonlinear singularly perturbed system as described by Theorem 11.4 of Khalil (2007). Substituting $\boldsymbol{\xi} = \dot{\boldsymbol{e}}$ into Eq. (17) leads to

$$\begin{aligned}\dot{\boldsymbol{x}}_2 = \ddot{\boldsymbol{e}} = -\boldsymbol{M}^{-1}[&\boldsymbol{K}_{\mathrm{p}}\mathrm{Atan}(\boldsymbol{K}_{\boldsymbol{e}}\boldsymbol{e}) + \boldsymbol{K}_{\mathrm{d}}\mathrm{Atan}(\boldsymbol{K}_{\xi}\dot{\boldsymbol{e}}) \\ &+ (\boldsymbol{C}+\boldsymbol{C}_{\mathrm{d}}+\boldsymbol{F}_{\mathrm{v}})\dot{\boldsymbol{e}}].\end{aligned} \tag{19}$$

Thus, we obtain the reduced system (slow model) (16) and (19), and the boundary-layer system (fast model)

$$\frac{\mathrm{d}\boldsymbol{y}}{\mathrm{d}\delta} = \frac{\mathrm{d}\boldsymbol{z}}{\mathrm{d}\delta} = \dot{\boldsymbol{e}} - \boldsymbol{\xi}, \tag{20}$$

where $\boldsymbol{y}=\boldsymbol{z}-\dot{\boldsymbol{e}}$, $\delta=t/\varepsilon$, and $\dot{\boldsymbol{e}}$ is recognized as a constant.

Proposition 1 For any initial state condition $[\boldsymbol{e}(0)^{\mathrm{T}}\ \dot{\boldsymbol{e}}(0)^{\mathrm{T}}\ \boldsymbol{\xi}(0)^{\mathrm{T}}]^{\mathrm{T}} \in \Phi_\eta$, where $\Phi_\eta=\{\boldsymbol{x}\in\mathbb{R}^{3n}: \|\boldsymbol{x}\| \le\eta\}$, and $\eta>0$ is arbitrarily large, if

$$\frac{k_{\mathrm{dm}}}{k_{\xi\mathrm{M}}} + \frac{f_{\mathrm{vm}}}{k_{\xi\mathrm{M}}^2} - k_{\mathrm{C}}\|\dot{\boldsymbol{q}}_{\mathrm{d}}\|_{\mathrm{M}}\left(\frac{\alpha}{k_{\xi\mathrm{m}}}\right)^2 > 0 \tag{21}$$

is satisfied, then there always exists $\varepsilon^*>0$ such that $\forall\varepsilon^*>\varepsilon$, the state space origin of system (16), (17), and (18) is exponentially stable.

Proof According to Theorem 11.4 of Khalil (2007) (see the Appendix), the exponential stability proof of the singularly perturbed system can be achieved by following the five steps below:

Step 1: From Eqs. (16), (17), and (18), we obtain $[\dot{\boldsymbol{e}}^{\mathrm{T}}\ \ddot{\boldsymbol{e}}^{\mathrm{T}}\ \dot{\boldsymbol{\xi}}^{\mathrm{T}}]^{\mathrm{T}}=[0\ 0\ 0]^{\mathrm{T}}$, when $[\boldsymbol{e}^{\mathrm{T}}\ \dot{\boldsymbol{e}}^{\mathrm{T}}\ \boldsymbol{\xi}^{\mathrm{T}}]^{\mathrm{T}}=[0\ 0\ 0]^{\mathrm{T}}$. Thus, Assumption 1 in Theorem 11.4 of Khalil (2007) is satisfied.

Step 2: When $\varepsilon=0$, we obtain the unique isolated root $\boldsymbol{\xi}=\dot{\boldsymbol{e}}$ of Eq. (18).

Step 3: We can easily find that the right sides of Eqs. (16), (17), and (18) and their partial derivatives up to the second order are bounded for $\boldsymbol{\xi}-\dot{\boldsymbol{e}}\in B_\rho$.

Step 4: Stability analysis of the reduced system. We can find that the state space origin $[\boldsymbol{e}^{\mathrm{T}}\ \dot{\boldsymbol{e}}^{\mathrm{T}}]^{\mathrm{T}}=\boldsymbol{0}$ is the unique equilibrium point of the reduced system (16) and (19). Design a Lyapunov function $V(t, \boldsymbol{e}, \dot{\boldsymbol{e}})$ (written as V for short):

$$V=\sum_{i=1}^{n}\int_0^{e_i}k_{\mathrm{p}i}\,\mathrm{atan}(k_{ei}e_i)\mathrm{d}e_i+\frac{1}{2}\dot{\boldsymbol{e}}^{\mathrm{T}}\boldsymbol{M}\dot{\boldsymbol{e}}+\upsilon\dot{\boldsymbol{e}}^{\mathrm{T}}\boldsymbol{M}\mathrm{Atan}(\boldsymbol{K}_e\boldsymbol{e}),\tag{22}$$

where the constant $\upsilon>0$ is small enough.

Using properties P2 and Q6, we obtain

$$\begin{aligned}V\geq&\frac{1}{2}\left(\frac{k_{\mathrm{p}i}}{k_{ei}}\right)_{\mathrm{m}}\|\mathrm{Atan}(\boldsymbol{K}_e\boldsymbol{e})\|^2+\frac{\lambda_{\mathrm{m}}\{\boldsymbol{M}\}\|\dot{\boldsymbol{e}}\|^2}{2}\\&-\upsilon\lambda_{\mathrm{M}}\{\boldsymbol{M}\}\|\dot{\boldsymbol{e}}\|\cdot\|\mathrm{Atan}(\boldsymbol{K}_e\boldsymbol{e})\|.\end{aligned}\tag{23}$$

Then, $\forall[\boldsymbol{e}^{\mathrm{T}}\ \dot{\boldsymbol{e}}^{\mathrm{T}}]^{\mathrm{T}}\in B_\eta$, $B_\eta=\{\boldsymbol{x}\in\mathbb{R}^{2n}: \|\boldsymbol{x}\|\leq\eta\}$, where η is as defined in Proposition 1, V is positive definite if

$$\upsilon<\upsilon_1=\frac{1}{\lambda_{\mathrm{M}}\{\boldsymbol{M}\}}\sqrt{2\gamma_1\lambda_{\mathrm{m}}\{\boldsymbol{M}\}\left(\frac{k_{\mathrm{p}i}}{k_{ei}}\right)_{\mathrm{m}}}.\tag{24}$$

By using the Newton-Leibniz formula, the time derivative of the first part on the right of Eq. (22) can be written as $\dot{\boldsymbol{e}}^{\mathrm{T}}\boldsymbol{K}_{\mathrm{p}}\mathrm{Atan}(\boldsymbol{K}_e\boldsymbol{e})$. Then the time derivative of V is given by

$$\begin{aligned}\dot{V}=&-\dot{\boldsymbol{e}}^{\mathrm{T}}[(\boldsymbol{C}_{\mathrm{d}}+\boldsymbol{F}_{\mathrm{v}})\dot{\boldsymbol{e}}+\boldsymbol{K}_{\mathrm{d}}\mathrm{Atan}(\boldsymbol{K}_\xi\dot{\boldsymbol{e}})]\\&+\upsilon\Bigg[\ddot{\boldsymbol{e}}^{\mathrm{T}}\boldsymbol{M}\mathrm{Atan}(\boldsymbol{K}_e\boldsymbol{e})+\dot{\boldsymbol{e}}^{\mathrm{T}}\dot{\boldsymbol{M}}\mathrm{Atan}(\boldsymbol{K}_e\boldsymbol{e})\\&+\dot{\boldsymbol{e}}^{\mathrm{T}}\boldsymbol{M}\frac{\partial\mathrm{Atan}(\boldsymbol{K}_e\boldsymbol{e})}{\partial\boldsymbol{e}}\dot{\boldsymbol{e}}\Bigg].\end{aligned}\tag{25}$$

According to properties P1–P4, Q1–Q6, and the inequality $\|\dot{\boldsymbol{q}}\|\leq\|\dot{\boldsymbol{e}}\|+\|\dot{\boldsymbol{q}}_{\mathrm{d}}\|$, we obtain

$$\begin{aligned}\dot{V}\leq&-\begin{bmatrix}\|\mathrm{Atan}(\boldsymbol{K}_e\boldsymbol{e})\|\\\|\mathrm{Atan}(\boldsymbol{K}_\xi\dot{\boldsymbol{e}})\|\end{bmatrix}^{\mathrm{T}}\boldsymbol{S}\begin{bmatrix}\|\mathrm{Atan}(\boldsymbol{K}_e\boldsymbol{e})\|\\\|\mathrm{Atan}(\boldsymbol{K}_\xi\dot{\boldsymbol{e}})\|\end{bmatrix}\\\leq&-\lambda_{\mathrm{m}}\{\boldsymbol{S}\}\left\|\left[\|\mathrm{Atan}(\boldsymbol{K}_e\boldsymbol{e})\|\ \ \|\mathrm{Atan}(\boldsymbol{K}_\xi\dot{\boldsymbol{e}})\|\right]^{\mathrm{T}}\right\|^2,\end{aligned}\tag{26}$$

where the entries of matrix $\boldsymbol{S}=\begin{bmatrix}s_{11}&s_{12}\\s_{21}&s_{22}\end{bmatrix}$ are

$$s_{11}=\upsilon k_{\mathrm{pm}},\ s_{12}=s_{21}=-\upsilon T_3,\ s_{22}=T_1-\upsilon T_2,$$

$$T_1=\frac{k_{\mathrm{dm}}}{k_{\xi\mathrm{M}}}+\frac{f_{\mathrm{vm}}}{k_{\xi\mathrm{M}}^2}-k_{\mathrm{C}}\|\dot{\boldsymbol{q}}_{\mathrm{d}}\|_{\mathrm{M}}\left(\frac{\alpha}{k_{\xi\mathrm{m}}}\right)^2,$$

$$T_2=\left(\frac{\sqrt{n}\pi k_{\mathrm{C}}}{2}+k_{e\mathrm{M}}\lambda_{\mathrm{M}}\{\boldsymbol{M}\}\right)\left(\frac{\alpha}{k_{\xi\mathrm{m}}}\right)^2,$$

$$T_3=\left(k_{\mathrm{C}}\|\dot{\boldsymbol{q}}_{\mathrm{d}}\|_{\mathrm{M}}+\frac{f_{\mathrm{vM}}}{2}\right)\left(\frac{\alpha}{k_{\xi\mathrm{m}}}\right)+\frac{k_{\mathrm{dM}}}{2}.$$

Specifically, if $\boldsymbol{S}$ is positive definite, then $\dot{V}$ is negative definite. Note that $s_{11}=\upsilon k_{\mathrm{pm}}>0$, by Sylvester's theorem, if the entries of $\boldsymbol{S}$ satisfy $s_{11}s_{22}-s_{12}^2>0$, i.e.,

$$0<\upsilon<\upsilon_2=\frac{k_{\mathrm{pm}}T_1}{k_{\mathrm{pm}}T_2+T_3^2},\tag{27}$$

then the positive definiteness of $\boldsymbol{S}$ is guaranteed.

Also, by properties P2, Q5, and Q6, and using the same method of obtaining Eq. (25), we can obtain

$$\begin{aligned}V\leq&\begin{bmatrix}\|\mathrm{Atan}(\boldsymbol{K}_e\boldsymbol{e})\|\\\|\mathrm{Atan}(\boldsymbol{K}_\xi\dot{\boldsymbol{e}})\|\end{bmatrix}^{\mathrm{T}}\boldsymbol{Q}\begin{bmatrix}\|\mathrm{Atan}(\boldsymbol{K}_e\boldsymbol{e})\|\\\|\mathrm{Atan}(\boldsymbol{K}_\xi\dot{\boldsymbol{e}})\|\end{bmatrix}\\\leq&\lambda_{\mathrm{M}}\{\boldsymbol{Q}\}\left\|\left[\|\mathrm{Atan}(\boldsymbol{K}_e\boldsymbol{e})\|\ \ \|\mathrm{Atan}(\boldsymbol{K}_\xi\dot{\boldsymbol{e}})\|\right]^{\mathrm{T}}\right\|^2,\end{aligned}\tag{28}$$

where $\boldsymbol{Q}\in\mathbb{R}^{n\times n}$ is a constant symmetric matrix.

Then, from Eqs. (26) and (28), we obtain

$$\dot{V} \le -\frac{\lambda_{\rm m}\{\boldsymbol{S}\}}{\lambda_{\rm M}\{\boldsymbol{Q}\}} V; \tag{29}$$

i.e., $\forall[\boldsymbol{e}^{\rm T}\ \dot{\boldsymbol{e}}^{\rm T}]^{\rm T}\in B_\eta$, the exponential stability of the reduced system (16) and (19) is assured, if $T_1>0$ (i.e., condition (21) is satisfied, and $0<\upsilon<\min\{\upsilon_1, \upsilon_2\}$).

Step 5: Stability analysis of the boundary-layer system. A Lyapunov function $W(\delta, \boldsymbol{\xi})$ (written as W for short) for system (20) is given as

$$W = \omega(\dot{\boldsymbol{e}} - \boldsymbol{\xi})^{\rm T}(\dot{\boldsymbol{e}} - \boldsymbol{\xi}), \tag{30}$$

where the constant $\omega>0$ is small enough.

Further, we obtain

$$\frac{{\rm d}W}{{\rm d}\delta} = -2\omega(\dot{\boldsymbol{e}} - \boldsymbol{\xi})^{\rm T}(\dot{\boldsymbol{e}} - \boldsymbol{\xi}) = -2W; \tag{31}$$

i.e., the boundary-layer system (20) is exponentially stable, uniformly in (t, $\boldsymbol{x}$), without any restriction. From system (31), we can find that, the smaller the ε is, the larger the scaled time variable $\delta=t/\varepsilon$ will be, and the faster exponential convergence the system (20) will have.

At this point, all five assumptions in Theorem 11.4 of Khalil (2000) are satisfied. Consequently, there always exists $\varepsilon^*>0$ such that $\forall\varepsilon^*>\varepsilon$ and $[\boldsymbol{e}(0)^{\rm T}\ \dot{\boldsymbol{e}}(0)^{\rm T}\ \boldsymbol{\xi}(0)^{\rm T}]^{\rm T}\in\Phi_\eta$, the exponential stability of system (16), (17), and (18) is guaranteed.

In Section 4.3, all the output values of $k_{{\rm p}i}$ and $k_{{\rm d}i}$ of the fuzzy self-tuning regulator should be restricted by Eqs. (14) and (21), which are the necessary constraints for ensuring the continuous stability of the overall system and the boundedness of the torque control inputs.

5 Simulation results

To verify the effectiveness of the proposed scheme, we present some simulation comparisons between our controller and those proposed in Loria and Ortega (1995) and Moreno-Valenzuela *et al.* (2008a) on a two-link direct-driven robot manipulator (Fig. 5).

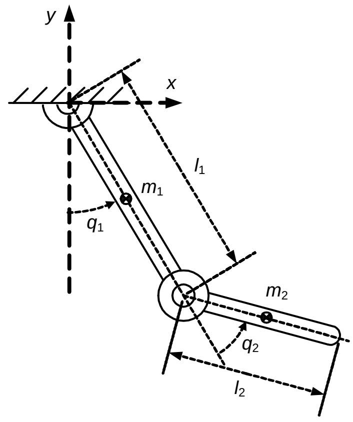

Fig. 5 A two-link direct-driven robot manipulator

The dynamic parameters are given as

$$\boldsymbol{M} = \begin{bmatrix} 3.3+0.24\cos q_2 & 0.11+0.12\cos q_2 \\ 0.11+0.12\cos q_2 & 0.11 \end{bmatrix},$$
$$\boldsymbol{C} = \begin{bmatrix} -0.12\dot{q}_2\sin q_2 & -0.12(\dot{q}_1+\dot{q}_2)\sin q_2 \\ 0.12\dot{q}_1\sin q_2 & 0 \end{bmatrix},$$
$$\boldsymbol{G} = \begin{bmatrix} 48.02\sin q_1 + 1.96\sin(q_1+q_2) \\ 1.96\sin(q_1+q_2) \end{bmatrix},$$
$$\boldsymbol{F}_{\rm v} = {\rm diag}\{2.5,\ 0.2\},\ \tau_{\rm 1M} = 120\ {\rm N\cdot m},\ \tau_{\rm 2M} = 20\ {\rm N\cdot m}.$$

The control law proposed in Moreno-Valenzuela *et al.* (2008a) (called M-S-C's) can be written as

$$\begin{aligned}\boldsymbol{\tau} &= \bar{\boldsymbol{K}}_{\rm p}{\rm Tanh}(\boldsymbol{K}_{\boldsymbol{e}}\boldsymbol{e}) + \bar{\boldsymbol{K}}_{\rm d}{\rm Tanh}(\boldsymbol{K}_{\xi}\boldsymbol{\xi}) \\ &\quad + \boldsymbol{M}\ddot{\boldsymbol{q}}_{\rm d} + (\boldsymbol{C}_{\rm d} + \boldsymbol{F}_{\rm v})\dot{\boldsymbol{q}}_{\rm d} + \boldsymbol{G},\end{aligned} \tag{32}$$

and the control law in Loria and Ortega (1995) (called L-O's) is

$$\boldsymbol{\tau} = \bar{\boldsymbol{K}}_{\rm p}\boldsymbol{e} + \bar{\boldsymbol{K}}_{\rm d}\boldsymbol{\xi} + \boldsymbol{M}\ddot{\boldsymbol{q}}_{\rm d} + (\boldsymbol{C}_{\rm d} + \boldsymbol{F}_{\rm v})\dot{\boldsymbol{q}}_{\rm d} + \boldsymbol{G}, \tag{33}$$

where $\boldsymbol{e}$ and $\boldsymbol{\xi}$ in each controller have the same relationship as described by Eq. (13), in which we select $\boldsymbol{U}$=diag{500, 500}, and $\bar{\boldsymbol{K}}_{\rm p}$ and $\bar{\boldsymbol{K}}_{\rm d}$ are the fixed PD gains.

To gain satisfactory tracking results and make fair comparison, we set the same PD gains in M-S-C's and L-O's: $\bar{\boldsymbol{K}}_{\rm p}$ =diag{4.5, 1.5}, $\bar{\boldsymbol{K}}_{\rm d}$ =diag{2, 0.2}. And, the same error gains in ours and M-S-C's: $\boldsymbol{K}_{\boldsymbol{e}}$=diag{3, 2}, $\boldsymbol{K}_{\xi}$=diag{3, 2}.

Without loss of generality, the desired position trajectories with non-zero initial position tracking errors for each joint are given as

$$q_{d1}(t)=\left[60\left(1-e^{-3t^3}\right)+20\left(1-e^{-3t^3}\right)\sin(6t)+10\right]^{\circ},$$
$$q_{d2}(t)=\left[75\left(1-e^{-2t^3}\right)+105\left(1-e^{-2t^3}\right)\sin(1.5t)+15\right]^{\circ}.$$

The parameters and fuzzy rules for the inference of the PD self-tuning regulator are set as shown in Tables 1–3, while the relationship surfaces of inputs and outputs are shown in Fig. 6. When selecting the physical universe of discourse of PD gains, from Eqs. (14) and (21), we can obtain these restrictions respectively as follows:

$$k_{p1}+k_{d1}<56.2,\quad k_{p2}+k_{d2}<7.8,$$
$$\min\{k_{d1},k_{d2}\}=k_{dm}>0.38.$$

Table 1 Parameters of the fuzzy PD regulator

Parameter	e_1, e_2 (°)	ξ_1, ξ_2 (°)	k_{p1}, k_{p2}	k_{d1}, k_{d2}
Physical universe of course	[−12, 12], [−12, 12]	[−15, 15], [−15, 15]	[2, 41], [1, 5.8]	[0.8, 14], [0.5, 1.7]
Quantization factor	1/4, 1/4	1/5, 1/5	2/13, 5/4	5/11, 5
Integer universe of course	{−3, −2, −1, 0, 1, 2, 3}			

Table 2 Fuzzy rules for k_{pi} for different e_i and ξ_i (i=1, 2)

e_i	Rule						
	ξ_i=NB	NM	NS	Z	PS	PM	PB
NB	PB	PB	PM	PM	PS	Z	Z
NM	PB	PB	PM	PS	PS	Z	NS
NS	PM	PM	PM	PS	Z	NS	NS
Z	PM	PM	PS	Z	NS	NM	NM
PS	PS	PS	Z	NS	NS	NM	NM
PM	PS	Z	NS	NM	NM	NM	NB
PB	Z	Z	NM	NM	NM	NB	NB

k_{p1} matches e_1, ξ_1; k_{p2} matches e_2, ξ_2

Table 3 Fuzzy rules for k_{di} for different e_i and ξ_i (i=1, 2)

e_i	Rule						
	ξ_i=NB	NM	NS	Z	PS	PM	PB
NB	PS	NS	NB	NB	NB	NM	PS
NM	PS	NS	NB	NM	NM	NS	Z
NS	Z	NS	NM	NM	NM	NS	Z
Z	Z	NS	NS	NS	NS	NS	Z
PS	Z	Z	Z	Z	Z	Z	Z
PM	PB	NS	PS	NM	PS	PS	PB
PB	PB	PM	PM	PM	PS	PS	PB

k_{d1} matches e_1, ξ_1; k_{d2} matches e_2, ξ_2

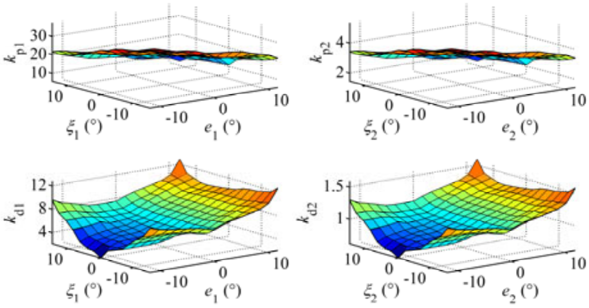

Fig. 6 Relationship surfaces of e_i, ξ_i, k_{pi}, and k_{di} (i=1, 2)

Furthermore, to test the anti-disturbance capability of the controllers, we applied man-made step torques as external disturbances during the 7th second with amplitudes of 0.6 N·m to the 1st joint and 0.2 N·m to the 2nd one.

The architecture comparison of our controller against those of M-S-C's and L-O's is shown in Table 4.

Table 4 Architecture comparison

Controller	Saturation function	Fuzzy self-tuning
Ours	atan	Has
M-S-C's	tanh	Has not
L-O's	Has not	Has not

M-S-C's: control law in Moreno-Valenzuela *et al*. (2008a); L-O's: control law in Loria and Ortega (1995)

To make overall appraisement to the performance of each controller, we adopt five criteria as follows:

Adjusting time—a period from the start to the moment tracking error e_i falls into the area of ±0.06°;

Overshoot—the maximum absolute value of e_i during the adjusting procedure;

Recovery time—a period from the end of disturbances to the moment tracking error e_i falls into the area of ±0.06°;

Maximum deviation—the maximum value of $|e_i|$ from the start of disturbances to the end of the recovery procedure;

RMS—root mean square, which is defined as

$$\mathrm{RMS}[e_i(t)]=\sqrt{\frac{1}{T}\int_0^T |e_i(t)|^2 \mathrm{d}t},\quad i=1,\ 2, \tag{34}$$

$$\mathrm{RMS}[\boldsymbol{e}(t)]=\sqrt{\frac{1}{T}\int_0^T \|\boldsymbol{e}(t)\|^2 \mathrm{d}t}. \tag{35}$$

As shown in Fig. 7 and Table 5, our controller had the shortest adjusting time and recovery time, the smallest overshoot, the maximum deviation, a relatively low RMS[$e_i(t)$], and the lowest value of RMS[$\boldsymbol{e}(t)$], representing superior capacity of dynamic response and anti-disturbance to those of M-S-C's and L-O's with continuous asymptotic stability. This is because we applied a fuzzy PD self-tuning regulator whose outputs, k_{pi} and k_{di}, are properly constrained by Eqs. (14) and (21), and invoked a wider range saturation function, arctangent.

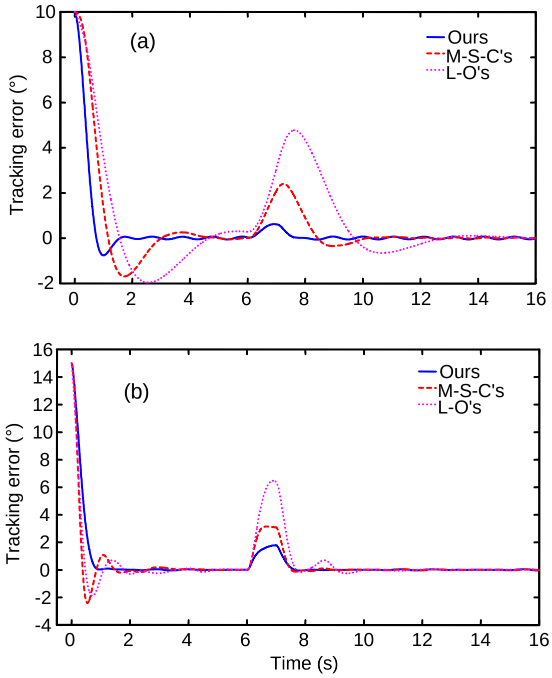

Fig. 7 Tracking errors of the first joint (a) and the second joint (b)

M-S-C's: control law in Moreno-Valenzuela *et al*. (2008a); L-O's: control law in Loria and Ortega (1995)

Table 5 Performance comparison

Parameter		Value		
		Ours	M-S-C's	L-O's
Adjusting time (s)	1st joint	1.5	4.4	>6.0
	2nd joint	0.9	3.5	4.8
Overshoot (°)	1st joint	0.76	1.69	1.97
	2nd joint	0.00	2.41	1.89
Recovery time (s)	1st joint	3.6	4.0	>7.7
	2nd joint	0.6	1.8	4.3
Maximum deviation (°)	1st joint	0.62	2.40	4.77
	2nd joint	1.79	3.14	6.47
RMS (°)	e_1	1.341	1.953	2.482
	e_2	1.804	1.688	2.050
	$\lVert\boldsymbol{e}\rVert$	2.248	2.581	4.439

M-S-C's: control law in Moreno-Valenzuela *et al*. (2008a); L-O's: control law in Loria and Ortega (1995)

Moreover, as shown in Figs. 8a and 8b, L-O's failed to keep the initial torque inputs in the given limited range, with peak torque control input values of about 132 N·m to the 1st joint and 26.7 N·m to the 2nd one, just for the reason that there is no saturation function in the control law to create bounded inputs as ours and M-S-C's did.

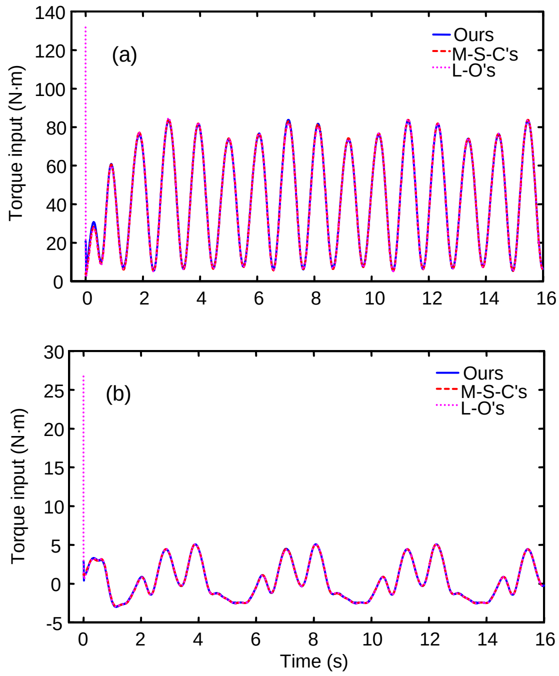

Fig. 8 Torque inputs of the first joint (a) and the second joint (b)

M-S-C's: control law in Moreno-Valenzuela *et al*. (2008a); L-O's: control law in Loria and Ortega (1995)

6 Conclusions

In this paper, a novel saturated OFT controller via fuzzy self-tuning has been developed for the trajectory tracking of robot manipulators. A modified arctangent saturation function is first invoked in the control law to ensure the boundedness of the torque inputs, and a linear filter is applied in the closed-loop control to eliminate the velocity measurements. A fuzzy strategy is used to make the PD gains vary as the position and pseudo velocity tracking errors change, which has greatly improved the dynamic performance of the tracking control.

In the stability analysis of the proposed closed-loop tracking system, the theory of singularly perturbed systems is applied. Based on this, proper restrictions on the range of PD gains are created to ensure the continuous semi-global exponential stability of the system during the self-tuning process. It is also worthwhile to mention that, by this method, we can decompose the design of the tracking system into two subsystems, both of which may be realized easily.

Simulation comparisons among our controller and others are implemented on a two-link direct-driven robot manipulator. The tracking results verify the effectiveness of the proposed saturated OFT controller, which achieves a better tracking performance than others.

References

Andrieu, V., Praly, L., 2009. A unifying point of view on output feedback designs for global asymptotic stabilization. *Automatica*, **45**(8):1789-1798. [doi:10.1016/j.automatica.2009.04.015]

Burkov, I.V., 1998. Stabilization of a natural mechanical system without measuring its velocities with application to the control of a rigid body. *J. Appl. Math. Mech.*, **62**(6):853-862. [doi:10.1016/S0021-8928(98)00109-9]

Dai, D., Hu, T.S., Teel, A.R., Zaccarian, L., 2009. Output feedback design for saturated linear plants using deadzone loops. *Automatica*, **45**(12):2917-2924. [doi:10.1016/j.automatica.2009.09.022]

Hernandez-Guzman, V.M., Santibanez, V., Silva-Ortigoza, R., 2008. A new tuning procedure for PID control of rigid robots. *Adv. Robot.*, **22**(9):1007-1023. [doi:10.1163/156855308X315154]

Hu, T.S., Teel, A.R., Zaccarian, L., 2008. Anti-windup synthesis for linear control systems with input saturation: achieving regional, nonlinear performance. *Automatica*, **44**(2):512- 519. [doi:10.1016/j.automatica.2007.06.003]

Kelly, R., Santibanez, V., 2005. Control of Robot Manipulators in Joint Space. Springer, Berlin.

Khalil, H.K., 2007. Nonlinear Systems. Publishing House of Electronics Industry, Beijing.

Li, W., Chang, X.G., Wahl, F.M., Farrell, J., 2001. Tracking control of a manipulator under uncertainty by fuzzy P+ID controller. *Fuzzy Sets Syst.*, **122**(1):125-137. [doi:10.1016/S0165-0114(00)00019-1]

Liu, H.S., Zhu, S.Q., 2009. A generalized trajectory tracking controller for robot manipulators with bounded inputs. *J. Zhejiang Univ.-Sci. A*, **10**(10):1500-1508. [doi:10.1631/jzus.A0820725]

Llama, M.A., Santibanez, V., Kelly, R., 1998. Stable Fuzzy Self-tuning Computed-Torque Control of Robot Manipulators. Proc. IEEE Int. Conf. on Robotics and Automation, p.2369-2374. [doi:10.1109/ROBOT.1988.680678]

Llama, M.A., Santibanez, V., Flores, J., 1999. A Passivity Based Stability Analysis for a Fuzzy PD+ Control for Robot Manipulators. Proc. 18th Int. Conf. of the North American Fuzzy Information Processing Society, p.665-669. [doi:10.1109/NAFIPS.1999.781777]

Llama, M.A., Kelly, R., Santibanez, V., 2001. A stable motion control system for manipulators via fuzzy self-tuning. *Fuzzy Sets Syst.*, **124**(2):133-154. [doi:10.1016/S0165-0114(00)00061-0]

Loria, A., Nijmeijer, H., 1998. Bounded output feedback tracking control of full actuated Euler-Lagrange systems. *Syst. Control Lett.*, **33**(3):151-161. [doi:10.1016/S0167-6911(97)80170-3]

Loria, A., Ortega, R., 1995. On tracking control of rigid and flexible joints robots. *Int. J. Appl. Math. Comput. Sci.*, **5**(2):101-113.

Meza, J.L., Santibanez, V., Campa, R., 2007. An estimate of the domain of attraction for the PID regulator of manipulators. *Int. J. Robot. Autom.*, **22**(3):187-195. [doi:10.2316/Journal.206.2007.3.206-2829]

Moreno-Valenzuela, J., Santibanez, V., Campa, R., 2008a. On output feedback tracking control of robot manipulators with bounded torque input. *Int. J. Control Autom. Syst.*, **6**(1):76-85.

Moreno-Valenzuela, J., Santibanez, V., Campa, R., 2008b. A class of OFT controllers for torque-saturated robot manipulators: Lyapunov stability and experimental evaluation. *J. Intell. Robot. Syst.*, **51**(1):65-88. [doi:10.1007/s10846-007-9181-6]

Park, J.K., Choi, C.H., 1995. Dynamic compensation method for multivariable control systems with saturating actuators. *IEEE Trans. Autom. Control*, **40**(9):1635-1640. [doi:10.1109/9.412636]

Santibanez, V., Kelly, R., 2001. Global Asymptotic Stability of Bounded Output Feedback Tracking Control for Robot Manipulators. Proc. 44th IEEE Conf. on Decision and Control, p.1378-1379. [doi:10.1109/2001.981082]

Santibanez, V., Kelly, R., Llama, M.A., 2000. Fuzzy PD+ Control for Robot Manipulators. Proc. IEEE Int. Conf. on Robotics and Automation, p.2112-2117. [doi:10.1109/ROBOT.2000.846341]

Santibanez, V., Kelly, R., Llama, M.A., 2005. A novel global asymptotic stable set-point fuzzy controller with bounded torques for robot manipulators. *IEEE Trans. Fuzzy Syst.*, **13**(3):362-372. [doi:10.1109/TFUZZ.2004.841735]

Santibanez, V., Kelly, R., Zavala-Rio, A., Parada, P., 2008. A New Saturated Nonlinear PID Global Regulator for Robot Manipulators. Proc. 17th IFAC Word Congress, p.11690-11695. [doi:10.3182/20080706-5-KR-1001.2637]

Yoon, S.S., Park, J.K., Yoon, T.W., 2008. Dynamic anti-windup scheme for feedback linearizable nonlinear control systems with saturating inputs. *Automatica*, **44**(12):3176-3180. [doi:10.1016/j.automatica.2008.10.003]

Appendix: Theorem 11.4 in Khalil (2007)

Consider the singularly perturbed system

$$\dot{\boldsymbol{x}} = f(t, \boldsymbol{x}, \boldsymbol{z}, \varepsilon), \tag{A1}$$

$$\varepsilon \dot{\boldsymbol{z}} = g(t, \boldsymbol{x}, \boldsymbol{z}, \varepsilon), \tag{A2}$$

where $\boldsymbol{x}\in\mathbb{R}^{n_1}$, $\boldsymbol{z}\in\mathbb{R}^{n_2}$, $\varepsilon>0$.

Assume the assumptions below are satisfied $\forall(t, \boldsymbol{x}, \varepsilon)\in[0, +\infty)\times B_\eta\times[0, \varepsilon_0]$, $B_\eta=\{\boldsymbol{x}\in\mathbb{R}^{n_1}: \|\boldsymbol{x}\|\leq\eta\}$:

1. $f(t, \mathbf{0}, \mathbf{0}, \varepsilon)=\mathbf{0}$ and $g(t, \mathbf{0}, \mathbf{0}, \varepsilon)=\mathbf{0}$.

2. The equation $g(t, \boldsymbol{x}, \boldsymbol{z}, \varepsilon)=\mathbf{0}$ has an isolated root $\boldsymbol{z}=h(t, \boldsymbol{x})$ such that $h(t, \mathbf{0})=\mathbf{0}$.

3. The functions f, g, h and their partial derivatives up to the second-order are bounded for $\boldsymbol{z}-h(t, \boldsymbol{x})\in B_\rho$, where $B_\rho=\{\boldsymbol{x}\in\mathbb{R}^{n_2}: \|\boldsymbol{x}\|\leq\rho\}$.

4. The origin of the reduced system

$$\dot{\boldsymbol{x}} = f(t, \boldsymbol{x}, h(t, \boldsymbol{x}), 0) \tag{A3}$$

is exponentially stable.

5. The origin of the boundary-layer system

$$\frac{\mathrm{d}\boldsymbol{y}}{\mathrm{d}\delta} = g(t, \boldsymbol{x}, \boldsymbol{y} + h(t, \boldsymbol{x}), 0) \tag{A4}$$

is exponentially stable, uniformly in $(t, \boldsymbol{x})$, where $\delta=t/\varepsilon$, and $\boldsymbol{y}=\boldsymbol{z}-h(t, \boldsymbol{x})$.

Then, there exists $\varepsilon^*>0$ such that $\forall\varepsilon^*>\varepsilon$, the origin of system (A1) and (A2) is exponentially stable.